OPEN ACCESS
IOP Publishing | Astro Ltd
Laser Physics Letters
Laser Phys. Lett. **16** (2019) 055202 (9pp)
https://doi.org/10.1088/1612-202X/ab0a60

Letter

Generation of stable, squeezed vacuum states at audio frequency using optical serrodyne sideband modulation locking method

Yinghao Gao[1], Jinxia Feng[1,2], Yuanji Li[1,2] and Kuanshou Zhang[1,2]

[1] State Key Laboratory of Quantum Optics and Quantum Optics Devices, Institute of Opto-Electronics, Shanxi University, Taiyuan 030006, People's Republic of China
[2] Collaborative Innovation Center of Extreme Optics, Shanxi University, Taiyuan 030006, People's Republic of China

E-mail: kuanshou@sxu.edu.cn

Received 3 February 2019
Accepted for publication 5 February 2019
Published 9 April 2019

Abstract

Squeezed vacuum states were generated using a subthreshold optical parametric oscillator (OPO) and a home-made, continuous-wave, single-frequency 532 nm and 1064 nm dual-wavelength laser. The OPO was pumped by the 532 nm output of the laser. The 1064 nm output of the laser was used to generate an auxiliary beam by optical serrodyne sideband modulation and a coherent control field (CCF). When the subthreshold OPO was locked using the auxiliary beam and the squeezing angle controlled using the CCF, 6.1 $\pm$ 0.3 dB phase-squeezed vacuum states at audio frequencies from 5 to 100 kHz were stably generated with a compact configuration.

Keywords: squeezed vacuum states, audio frequency, optical serrodyne sideband modulation

(Some figures may appear in colour only in the online journal)

1. Introduction

Squeezed vacuum states are an important tool for improving the sensitivity of laser interferometers, such as with gravitational wave (GW) detection [1–3]. They are also important resources for quantum information, quantum imaging and quantum enhanced high-precision measurements [4–7]. For practical applications of squeezed vacuum states, it is essential to obtain stable, squeezed vacuum states with high squeezing degrees and compact configurations. Squeezed vacuum states are commonly produced via a subthreshold optical parametric oscillator (OPO) in continuous variables systems [8–12]. So far, 15 dB squeezed vacuum states at Fourier frequencies from 3 to 8 MHz have been measured using a semi-monolithic OPO cavity [13]. However, it is difficult to obtain stable, squeezed vacuum states if the subthreshold OPO cavity is uncontrolled due to mechanical disturbances to the OPO cavity. Consequently, the length of the subthreshold OPO cavity needs to be locked to the main laser at the frequency of ω_0 [14]. Injection locking schemes rely on an injection of a weak, phase-modulated light into the subthreshold OPO at the frequency ω_0 [15]. The injected light has the same mode and polarization as the generated squeezed vacuum states, thereby turning the OPO into an optical parametric amplifier (OPA), and bright squeezed states are generated instead of squeezed vacuum

states. It has been shown that even the lowest carrier powers of injected light can introduce large amounts of excess noise at audio frequencies and that the squeezing degree of squeezed vacuum states will be reduced or even not achieved [16]. To obtain stable, squeezed vacuum states and avoid any contamination of the squeezed light by laser noise in the audio band, an auxiliary beam polarised orthogonally to the squeezed vacuum field needs to be used to lock the length of the subthreshold OPO cavity and spatially separated from the squeezed vacuum states with a polarised beam splitter (PBS) behind the OPO. The *p*-polarised auxiliary beam must be frequency shifted by employing a tunable laser to realise simultaneous resonance with the *s*-polarised squeezed vacuum field [17, 18]. Stable, squeezed vacuum states in the GW detection band were achieved in 2006 [17]. In their experiment, an auxiliary laser source with *p*-polarization and which was frequency shifted by about 1.4 GHz was used to lock the length of subthreshold OPO cavity. In 2011, the squeezed-light enhancement of GEO600 was demonstrated by employing squeezed vacuum states, and stable, squeezed vacuum states were achieved by using two auxiliary laser sources that frequency shifted several MHz to lock the cavity length of the squeezing resonator and control the phase of squeezed field, separately [18]. However, in this scheme, the auxiliary laser can provide a large frequency shift but it has to be phase locked to the main laser, and the level of squeezing measured will be reduced because of the relative frequency noise between the main and auxiliary lasers. It is well known that the electro-optical phase modulator (EOPM) can be used to transfer carrier power into sidebands and that the propagation direction of light at sideband frequency is the same as that of the carrier light. In particular, the fibre-based, waveguide-type EOPM has a typical bandwidth of up to dozens of GHz, and optical serrodyne sideband modulation allows one to achieve a wideband frequency shift of high efficiency [19, 20]. It is possible that the subthreshold OPO cavity length can be controlled with an auxiliary beam that is generated directly by transferring the main laser's power to the sidebands based on serrodyne sideband modulation technique via a fibre-based, waveguide-type EOPM; stable, squeezed vacuum states with compact configurations can be realised without an auxiliary laser source.

In addition, for practical applications such as nonclassical improvement of an interferometer's signal-to-noise ratio (SNR), the squeezing angle of squeezed vacuum states needs to be controlled for and locked to the modulation signal of interest. Controlling the squeezing angle of squeezed vacuum states is more challenging. The coherent control technique has emerged as the preferred means for solving this problem [17, 21, 22]. In this technique, a coherent locking field (CLF) has been used to control the squeezing angle, and the frequency of CLF is shifted out of the squeezing band to prevent any contamination of the squeezed field in the frequencies of interest. Since the CLF is coherent with the squeezed mode, its phase can be used as the reference for the squeezing angle. The CLF can be generated by passing a beam at the fundamental frequency through a single acousto-optic modulator (AOM) [17] or by using an auxiliary laser source [21]. In 2016, a CLF auxiliary beam produced by shifting the frequency of main laser using two AOMs was used to lock the squeezing angle of squeezed vacuum states [22]. In their experiment, a subthreshold triply resonant OPO was utilised and the cavity length was locked using a pump beam. The scheme using two AOMs has the advantage that an arbitrary frequency-detuned CLF can be obtained without contamination by a noticeable amount of light at the carrier frequency.

In this paper, stable, squeezed vacuum states at audio frequency were generated from a subthreshold doubly resonant OPO pumped by a home-made, continuous-wave (cw), single-frequency, dual-wavelength Nd:YVO_4/LBO laser. The subthreshold OPO cavity was locked using an auxiliary beam that was generated by shifting the frequency of the fundamental laser utilising optical serrodyne sideband modulation method via a fibre-based, waveguide-type EOPM and a nonlinear transmission line (NLTL). Furthermore, the squeezing angle of squeezed vacuum states was controlled with the coherent control technique using the fundamental laser whose frequency is shifted by two AOMs, and the noise distribution of the squeezed vacuum states in phase space was analysed theoretically and experimentally.

2. Theoretical description

2.1. Auxiliary beam frequency shifted by optical serrodyne sideband modulation

To lock a subthreshold OPO cavity, an auxiliary beam is needed. The auxiliary beam can be generated by transferring the fundamental laser power to the sidebands based on the optical serrodyne sideband modulation technique via a fibre-coupled EOPM. The electric field of the laser modulated by the EOPM that is driven by a periodic phase-modulated signal is given by

$$E(t) = E_0 \exp\left\{i\omega_0 t + \varphi(\omega_m t)\right\}, \tag{1}$$

where $\varphi(\omega_m t)$ is phase modulating function and ω_m is the angular frequency of the periodic phase-modulated signal. E_0 and ω_0 are the amplitude and angular frequency of the input laser field, respectively. When the laser is modulated by the EOPM driven by a sawtooth modulation function, the electric field can be written as [23]

$$E(t) = E_0 \exp(i\omega_0 t) \cdot \sum b_n \exp(in\omega_m t), \tag{2}$$

where $n = 0, \pm 1, \pm 2, \cdots$ represents n-order sideband and b_n is the Fourier coefficient of sawtooth phase-modulated function that is given by

$$b_n = \frac{1}{2\pi}\int_{-\pi}^{\pi} \exp i(\varphi(x) - nx)dx. \tag{3}$$

When the sawtooth modulation function is described as $\varphi(\omega_m t)$ with a peak phase deviation of $\delta\varphi$ and a width of the fly-back period of $2(\pi - \alpha)$ as shown in Figure 1(a), the Fourier coefficients of equation (3) can be written as

$$b_n = \frac{\alpha \sin(\delta\varphi - n\alpha)}{\pi(\delta\varphi - n\alpha)} + \frac{(\pi - \alpha)\sin(\delta\varphi - n\alpha)}{\pi(\delta\varphi + n(\pi - \alpha))}. \tag{4}$$

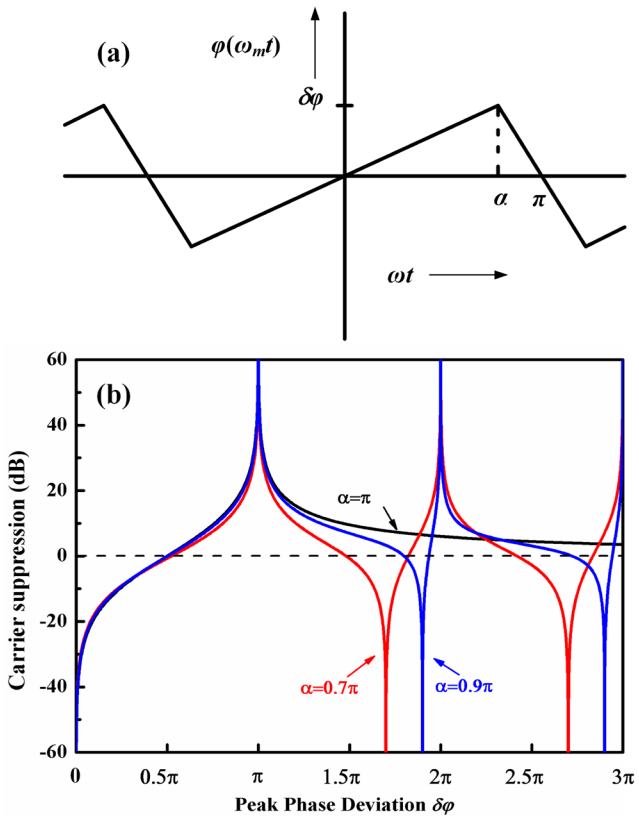

Figure 1. (a) Sawtooth phase modulation function with a peak phase deviation $\delta\varphi$ and a width $2(\pi-\alpha)$ of the fly-back. (b) Suppression of the carrier frequency dependent on the peak phase deviation $\delta\varphi$ with $\alpha = 0.7\pi$, $\alpha = 0.9\pi$, $\alpha = \pi$.

If only considering sidebands on the orders of 0 and ±1 and ignoring the contributions of higher-order terms, the electric field of the laser can be simplified as

$$E(t) \approx E_0 \exp(i\omega_0 t)[b_0 + b_1 \exp(i\omega_m t) + b_{-1}\exp(-i\omega_m t)]. \quad (5)$$

If the first-order sidebands of the p-polarised auxiliary beam frequency shifted by the optical serrodyne sideband modulation can be simultaneously resonant with the generated s-polarised squeezed state in the OPO cavity, it can be used to lock the length of the OPO cavity, and s-polarised squeezed vacuum states can be generated from a subthreshold OPO stably. When the carrier suppression is defined as $(|b_1|/|b_0|)^2$ or $(|b_{-1}|/|b_0|)^2$, it should be as large as possible to get a high SNR from the locking system. Therefore, the power transfer efficiency from the carrier frequency to the first-order sideband frequency that can be calculated using equation (4) is expected to be as high as possible. Whether to choose the upper or lower sideband as the p-polarised auxiliary beam depends on which frequency is closer to the resonant frequency of s-polarised beam in the OPO cavity. Figure 1(b) depicts the carrier suppression for the upper first-order sideband frequency depends on the peak phase deviation $\delta\varphi$ with different sawtooth phase modulation (α) of 0.7π, 0.9π and π, respectively. It was observed that the calculated maximum carrier suppression is 324 dB with a power transfer efficiency of 43% for $\delta\varphi = \pi$ with $\alpha = 0.7\pi$, the calculated maximum carrier suppression is 327 dB with a power transfer efficiency of 80% for $\delta\varphi = \pi$ with $\alpha = 0.9\pi$ and the calculated maximum carrier suppression is ∞ dB with a power transfer efficiency of 100% for $\delta\varphi = \pi$ with $\alpha = \pi$. Because an ideal sawtooth waveform with $\alpha = \pi$ cannot be generated in the experiment, the best choice is α to be 0.9π to obtain higher power transfer efficiency. Compared with the sinusoidal phase modulation in which the power transfer efficiency of the first-order sideband is about 34%, optical serrodyne sideband modulation can provide higher power transfer efficiency with a wideband frequency shift.

2.2. Control of the squeezing angle and analysis of the noise distribution of squeezed vacuum states

When a coherent control field (CCF) frequency shifted by a frequency of Ω with respect to the fundamental laser frequency (ω_0) is injected into the subthreshold OPO cavity and the relative phase between the pump field and CCF is locked, the control of squeezing angle of squeezed vacuum states can be realised. Note that Ω should be out of the squeezing band in the frequencies of interest but within the bandwidth of the OPO cavity. The outgoing CCF from the subthreshold OPO can be written as [24]

$$E^{CCF}(t) = \frac{g+1}{\sqrt{2g}}\beta_+^{in}\cos(\omega_0+\Omega)t + \frac{g-1}{\sqrt{2g}}\beta_+^{in}\cos((\omega_0-\Omega)t-2\theta), \quad (6)$$

where β_+^{in} represents real valued amplitude of CCF prior to any nonlinear interaction. $g = e^{2r}$, r refers to squeezing factor, and θ refers to squeezing angle.

The photocurrent from the photodetector is given by

$$I^{CCF}(t) = \left(\frac{g+1}{\sqrt{2g}}\beta_+^{in}\right)^2 + \left(\frac{g-1}{\sqrt{2g}}\beta_+^{in}\right)^2 + 2\left(\frac{g+1}{\sqrt{2g}}\beta_+^{in}\right)\left(\frac{g-1}{\sqrt{2g}}\beta_+^{in}\right)\cos(2\Omega t+2\theta). \quad (7)$$

After the photocurrent is finally mixed with an electrical demodulation signal $\beta_{\mathrm{demod1}}\cos(2\Omega t+\chi_1)$, a demodulation frequency of 2Ω, an amplitude of β_{demod1} and demodulation phase of χ_1, the alternating currents (AC) part of photocurrent with the higher-order terms ignored that can be used as the error signal to lock the squeezing angle is expressed as

$$\varepsilon = \frac{g^2-1}{2g}(\beta_+^{in})^2\beta_{\mathrm{demod1}}\cos(2\theta-\chi_1). \quad (8)$$

It can be seen that the error signal depends on the squeezing angle and demodulation phase χ_1. The zero point of ε can be changed by changing χ_1, and thus the signal ε can be directly used to control and lock the squeezing angle θ.

It is challenging to analyse the noise distribution of the squeezed vacuum states in phase space. Since the coherent amplitude of vacuum squeezed states is zero, the squeezing angle cannot be detected directly by balanced homodyne detectors (BHDs). If a CCF is injected into the subthreshold OPO cavity, thereby the OPO is turned into an OPA and bright squeezed states are generated at a Fourier frequency of

Ω. The generated bright squeezed states, copropagating with the squeezed vacuum states, are detected by the BHD with the local oscillator (LO) field. Consequently, the squeezing angle of squeezed vacuum states can be determined by controlling that of the bright squeezed states at a Fourier frequency of Ω. Furthermore, the noise distribution of the generated squeezed states in phase space can be analysed by scanning the relative phase between the CCF and LO when the squeezing angle is locked. The photocurrent subtraction of the BHD can be written as [25]

$$I_-(t) = 2\frac{g+1}{\sqrt{2g}}\beta_{LO}\beta_+^{in}\cos(\Omega t + \phi(t)) + 2\frac{g-1}{\sqrt{2g}}\beta_{LO}\beta_+^{in}\cos(\Omega t - \phi(t) + 2\theta), \quad (9)$$

where β_{LO} is the amplitude of the LO, and $\phi(t)$ is the relative phase between the CCF and LO.

Through linearizing annihilation and creation operators of quantum modes, the fluctuation of the photocurrent subtraction of the BHD can be written as

$$\delta I_-(t) = \beta_{LO}\begin{pmatrix}\delta\hat{X}^{out}(\Omega)\cos(\Omega t + \phi(t)) \\ +\delta\hat{Y}^{out}(\Omega)\sin(\Omega t + \phi(t))\end{pmatrix}, \quad (10)$$

where $\delta\hat{X}^{out}(\Omega)$ and $\delta\hat{Y}^{out}(\Omega)$ are the amplitude quadrature and phase quadrature fluctuations of output field from the OPO at frequency of $\omega_0 + \Omega$, respectively, and they can be given by

$$\delta\hat{X}^{out}(\Omega) = (\cosh(r) + \sinh(r)\cos(2\theta))\delta\hat{X}^{in}(\Omega) + \sinh(r)\sin(2\theta)\delta\hat{Y}^{in}(\Omega), \quad (11)$$

$$\delta\hat{Y}^{out}(\Omega) = \sinh(r)\sin(2\theta)\delta\hat{X}^{in}(\Omega) + (\cosh(r) - \sinh(r)\cos(2\theta))\delta\hat{Y}^{in}(\Omega), \quad (12)$$

where $\delta\hat{X}^{in}(\Omega)$ and $\delta\hat{Y}^{in}(\Omega)$ are the amplitude quadrature and phase quadrature fluctuations of the input CCF, respectively.

The noise distribution of the squeezed states in phase space can be analysed by phase synchronous detection with a mixer demodulator. The mixer is gated by a demodulation signal $\beta_{\text{demod2}}\cos(\Omega t + \chi_2)$, where β_{demod2} and χ_2 are the amplitude and phase of the demodulation signal, respectively. The amplitude of the noise current for a fixed squeezing angle θ at a Fourier frequency of Ω can be written as

$$I_-(t)|_\Omega = \frac{g+1}{\sqrt{g}}\beta_{LO}\beta_+^{in}\beta_{\text{demod2}}\cos(\phi(t) - \chi_2) + \frac{g-1}{\sqrt{g}}\beta_{LO}\beta_+^{in}\beta_{\text{demod2}}\cos(2\theta - \phi(t) - \chi_2). \quad (13)$$

Note that the higher-order terms in equation (13) are ignored. The signal $I_-(t)|_\Omega$ can be used to control and lock the relative phase between the generated squeezed fields and LO.

The fluctuation of noise current for a fixed squeezing angle θ at a Fourier frequency of Ω can be given by

$$\delta I_-(t)|_\Omega = \beta_{LO}\beta_{demod2}\begin{pmatrix}\delta\hat{X}^{out}(\Omega)\cos(\phi(t) - \chi_2) \\ +\delta\hat{Y}^{out}(\Omega)\sin(\phi(t) - \chi_2)\end{pmatrix}. \quad (14)$$

Equation (14) gives the noise distribution of squeezed states at a Fourier frequency of Ω. Generally, to simplify the analysis of the noise distribution, the phase of the demodulation signal is set to $\cos(\chi_2) = 1$. When the CCF at frequency of $\omega_0 + \Omega$ is injected into subthreshold OPO as the signal and the pump field is blocked, the output field will be in a coherent state. The amplitude is proportional to β_+^{in} and the fluctuation corresponds to the vacuum fluctuation. When the pump field is injected, and the relative phase of the pump and the CCF is fixed to $\pi/2$, the subthreshold OPO will be operated in the state of anti-amplification, and the amplitude squeezed vacuum states can be obtained. In this case, a bright amplitude squeezed state at a Fourier frequency of Ω is generated simultaneously, and the amplitude of the squeezed state is proportional to $e^{-r}\beta_+^{in}(r > 0)$, which is smaller than β_+^{in}. When $\phi = \pm n\pi$ ($n = 0, 1, 2, \ldots$), the noise amplitude of the squeezed state is proportional to $\delta\hat{X}^{out}(\Omega) = e^{-r}$, which is smaller than 1; i.e. it is smaller than that of the coherent state. When $\phi = \pm n\pi + \pi/2$ ($n = 0, 1, 2, \ldots$), the noise amplitude of the squeezed state is proportional to $\delta\hat{Y}^{out}(\Omega) = e^{r}$ that is larger than 1; i.e. it is larger than that of the coherent state. When the relative phase of the pump and the CCF is fixed to 0, the subthreshold OPO is operated in the state of amplification and the phase-squeezed vacuum states can be obtained. In this case, a bright phase-squeezed state at a Fourier frequency of Ω is generated simultaneously, and the amplitude of the squeezed state is proportional to $e^{r}\beta_+^{in}$ ($r > 0$), which is larger than β_+^{in}. When $\phi = \pm n\pi + \pi/2$ ($n = 0, 1, 2, \ldots$), the noise amplitude of the squeezed state is proportional to $\delta\hat{Y}^{out}(\Omega) = e^{-r}$, which is smaller than 1; i.e. it is smaller than that of the coherent state. When $\phi = \pm n\pi$ ($n = 0, 1, 2, \ldots$), the noise amplitude of the squeezed state is proportional to $\delta\hat{X}^{out}(\Omega) = e^{r}$, which is larger than 1; i.e. it is larger than that of the coherent state. Furthermore, the noise distribution of squeezed states in an arbitrary quadrature can be performed in phase space by controlling the relative phase of the pump and the CCF.

3. Experimental setup

The schematic diagram of the experimental setup for generation of stable, squeezed vacuum states is shown in Figure 2. The laser source was a home-made, low-noise, cw, single-frequency, dual-wavelength 532 nm and 1064 nm laser with an output power of 7 W at 532 nm and 3 W at 1064 nm. The infrared laser was sent through a ring mode cleaner (MC1) cavity with a finesse of 300 and linewidth of 1.0 MHz for preliminary filtering of the spatial mode and extra intensity noise of the laser.

The power of the green laser, acting as the OPO's pump, was stabilised using a Mach–Zehnder interferometer (MZI). The MZI was composed of two high-reflectivity (HR) mirrors ($R_{532\text{ nm}} > 99.8\%$) and two beam splitters ($R_{532\text{ nm}} = 90\%$). The green laser output from the MZI was sent to MC2 with a finesse of 270 and linewidth of 1.1 MHz in order to filter the laser's spatial mode and extra intensity noise. The two MCs' cavities were locked using the Pound–Drever–Hall (PDH) technique. The power transmittances of the two MCs

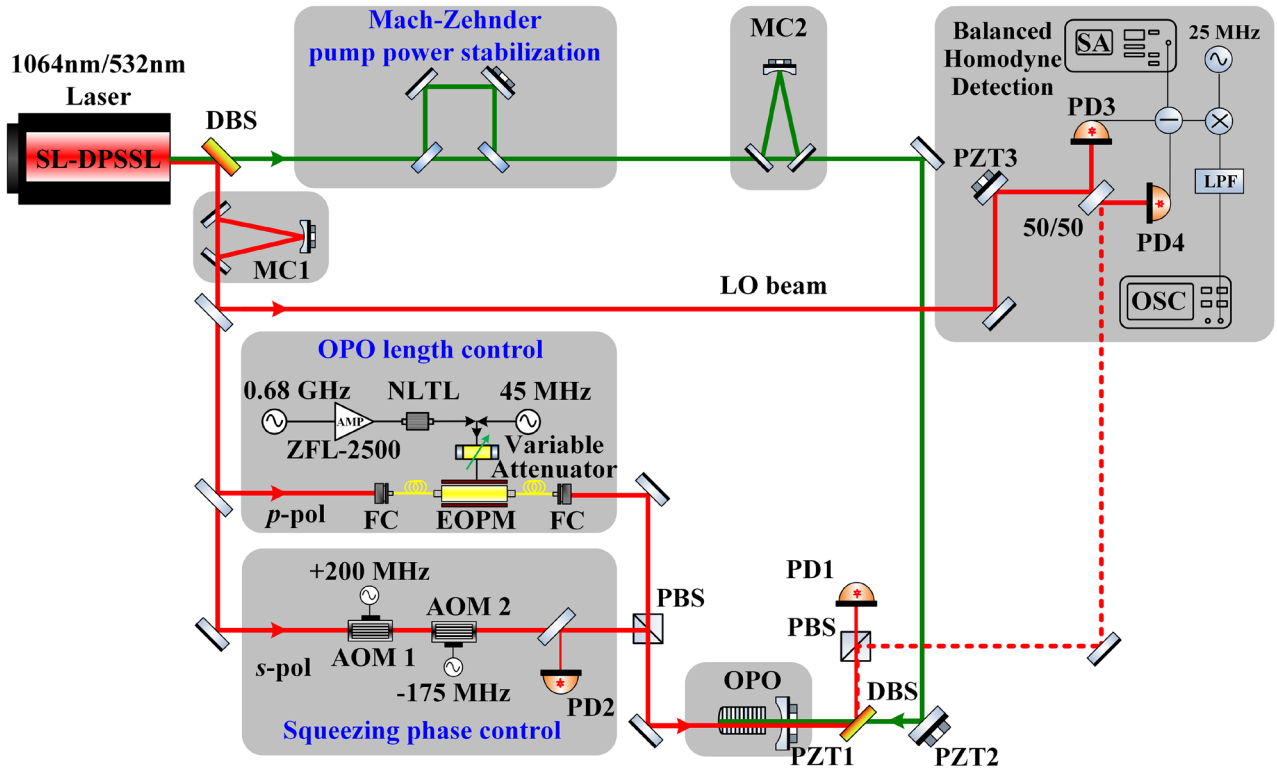

Figure 2. Schematic of the experimental setup for generation of stable, squeezed vacuum states. MC1: mode cleaner of 1064 nm; MC2: mode cleaner of 532 nm; NLTL: nonlinear transmission line; FC: fibre coupler; EOPM: electro-optical phase modulator; AOM: acousto-optic modulator; OPO: optical parametric oscillator; DBS: dichroic beam splitter; PD: photodiode; PBS: polarization beam splitter; PZT: piezo-electric transducer; ⊖: negative power combiner; ⊗: mixer; LPF: low pass filter; SA: spectrum analyser; OSC: oscilloscope.

were 78%. A portion of the output from MC1 was used as the LO beam of the BHD. The rest of the output from MC1 was used to generate the auxiliary beam and the CCF beam. The auxiliary beam was used to lock the subthreshold OPO cavity. The CCF beam was used to lock the relative phase between the pump field and CCF, as well as the relative phase between the LO field and CCF. The OPO was a semi-monolithic cavity composed of a PPKTP crystal with dimensions of 1 mm × 2 mm × 10 mm and a concave mirror with a radius of 25 mm. The concave face of the concave mirror acted as input and output couplers, and was partial transmission coated at 1064 nm and 532 nm ($T_{1064\ \mathrm{nm}} = 13\%$ & $T_{532\ \mathrm{nm}} = 80.0\%$). The flat face of the concave mirror was antireflection (AR) coated at 1064 nm and 532 nm ($R_{1064\ \&\ 532\ \mathrm{nm}} < 0.2\%$). One end of the PPKTP crystal was a convex surface with a radius of 12 mm, and was HR coated at 1064 nm and 532 nm ($R_{1064\ \&\ 532\ \mathrm{nm}} > 99.9\%$). The other end of the PPKTP crystal was flat, and was AR coated at 1064 nm and 532 nm ($R_{1064\ \&\ 532\ \mathrm{nm}} < 0.2\%$). The OPO was doubly resonant, and the pump was double passed through the cavity. The advantages of the doubly resonant OPO are that it is easier to operate than the triply resonant OPO and the absorption of PPKTP for 532 nm pump light is relatively smaller, which can decrease the vibration of the cavity length due to the change of the crystal temperature. The concave mirror was mounted on a piezo-electric transducer (PZT1) to control the length of the OPO cavity. The PPKTP crystal was housed in a copper oven and was temperature controlled by a home-made temperature controller with an accuracy of 0.01 °C. The temperature of PPKTP was kept at 40.0 °C in order to achieve optimum phase matching. The length of the OPO cavity was 37 mm, which led to a linewidth of 102 MHz and a free spectral range of 4.6 GHz. When the pump power was below the threshold of the OPO, squeezed vacuum states were generated. The *s*-polarised squeezed vacuum states from the subthreshold OPO were separated from the residual pump field by a dichroic beam splitter (DBS).

A portion of 1064 nm laser from MC1 passed through a fibre-based, waveguide-type EOPM (PM-0K5-10-PFA-1064, EOSPACE), and an auxiliary beam was generated by transferring 1064 nm laser power to the first-order sidebands. The EOPM was driven by a sawtooth signal, and high transfer efficiency with wideband frequency shift can be achieved. The sawtooth signal was generated by an NLTL (model 7103, Metelics). The NLTL was driven by a sinusoidal signal that was amplified using an amplifier (ZFL-2500VH + , Mini-circuits). The NLTL is essentially a ladder of inductors and semiconductor diodes which function as voltage-variable capacitors [26]. When a sinusoidal wave propagates through an NLTL, the higher-voltage parts of the signal propagate faster than the lower-voltage parts. This dispersion distorts the sinusoidal waveform, and an approximate sawtooth waveform can be obtained. A variable attenuator was used to adjust the amplitude of the sawtooth waveform. The efficiency of optical serrodyne sideband modulation can be optimised by adjusting the phase deviation and the width of the fly-back period of the sawtooth waveform. The *p*-polarised auxiliary beam was injected into the subthreshold OPO cavity. By adjusting the frequency of the sinusoidal signal, the auxiliary beam can

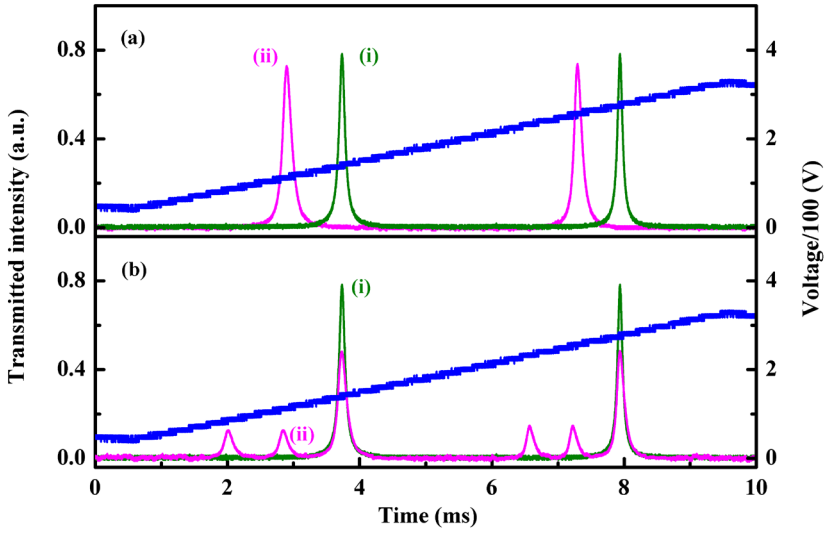

Figure 3. Transmitted intensity of lasers when the cavity was scanned. Without (a) and with (b) optical serrodyne sideband modulation. Curve (i): transmitted intensity of the *s*-polarised laser. Curve (ii): transmitted intensity of the *p*-polarised laser.

be simultaneously resonant with the generated *s*-polarised squeezed field in the cavity. The transmission of the auxiliary beam from the OPO was spatially separated with the squeezed vacuum field by a PBS and was detected by a photodiode (PD1). The subthreshold OPO cavity was locked using the PDH technique with a radio frequency of 45 MHz via the *p*-polarised auxiliary beam.

Another portion of the 1064 nm laser from MC1 passed through two AOMs. The first one was used to shift the frequency of the 1064 nm laser beam at 200 MHz. The second one was used to shift the frequency of the beam at −175 MHz. The CCF beam was generated by frequency shifting the 1064 nm laser to a frequency of $\Omega = 25$ MHz. When the CCF at the frequency of $\omega_0 + \Omega$ was injected into the subthreshold OPO that was pumped by 532 nm laser, a second sideband at $\omega_0 - \Omega$ was produced via difference frequency generation. The outgoing CCF from the subthreshold OPO was detected by PD2. After the photocurrent from PD2 was demodulated by a sinusoidal signal with a frequency of 50 MHz, the AC part of photocurrent was used as the error signal and fed back to PZT2 to lock the relative phase between the pump field and CCF, i.e. to lock the squeezing angle of the generated squeezed states.

The noise power of the down-conversion fields from the subthreshold OPO was measured by the BHD system. The down-conversion fields and LO were combined at a 50/50 beam splitter and detected by a pair of InGaAs photodiodes (PD3 and PD4). The photocurrents from PD3 and PD4 were combined by the negative power combiner. The AC part of photocurrent subtraction was recorded by a spectrum analyser (SA; N9030A, Agilent). The noise power of the down-conversion fields was analysed in frequency domain. To analyse the noise distribution of the down-conversion fields in time domain, the AC part of photocurrent subtraction was demodulated by a radio frequency signal with frequency of 25 MHz, filtered by a low-pass filter (LPF) with bandwidth of 1.9 MHz, and recorded by an oscilloscope (OSC; DPO 4054, Tektronix). This demodulated and filtered current was also used as the error signal and fed back to PZT3 to lock the relative phase between the CCF and LO, i.e. to lock the relative phase between the LO beam and squeezed vacuum states. The generated squeezed vacuum states can be measured continuously for a long time.

4. Results and discussion

When a *p*-polarised 1064 nm laser and an *s*-polarised 1064 nm laser were injected into the subthreshold OPO with a PPKTP crystal in the cavity, they were unable to resonate simultaneously in the cavity. The transmission of the 1064 nm lasers when the cavity length was scanned are shown in Figure 3(a); the measured frequency-shifting value between the *p*-polarised and *s*-polarised 1064 nm lasers was 0.68 GHz. When the NLTL was driven by a sinusoidal signal with a frequency of 0.68 GHz, and choosing the sawtooth phase modulation of $\alpha = 0.9\pi$ and peak phase deviation of $\delta\varphi = \pi$, respectively, the power of the *p*-polarised 1064 nm laser was transferred to the upper first-order sideband based on the optical serrodyne sideband modulation technique via a fibre-based, waveguide-type EOPM with a transfer efficiency of 66.4%. The transmissions of the *s*-polarised 1064 nm laser, *p*-polarised 1064 nm laser and first-order sidebands are shown in Figure 3(b). It can be seen that most of the power of the *p*-polarised 1064 nm laser was transferred to the upper first-order sideband and that the transmission of the upper first-order sideband overlapped with that of the *s*-polarised 1064 nm laser. The length of the subthreshold OPO cavity was locked by the frequency-shifted auxiliary beam using the PDH technique, and squeezed vacuum states can be generated stably.

Since the absorption coefficient of PPKTP is relatively large for 532 nm pump light, any pump power fluctuation will result in a change of crystal temperature and thus a change of the optical cavity length. While the subthreshold OPO cavity length was locked using the *p*-polarised auxiliary beam,

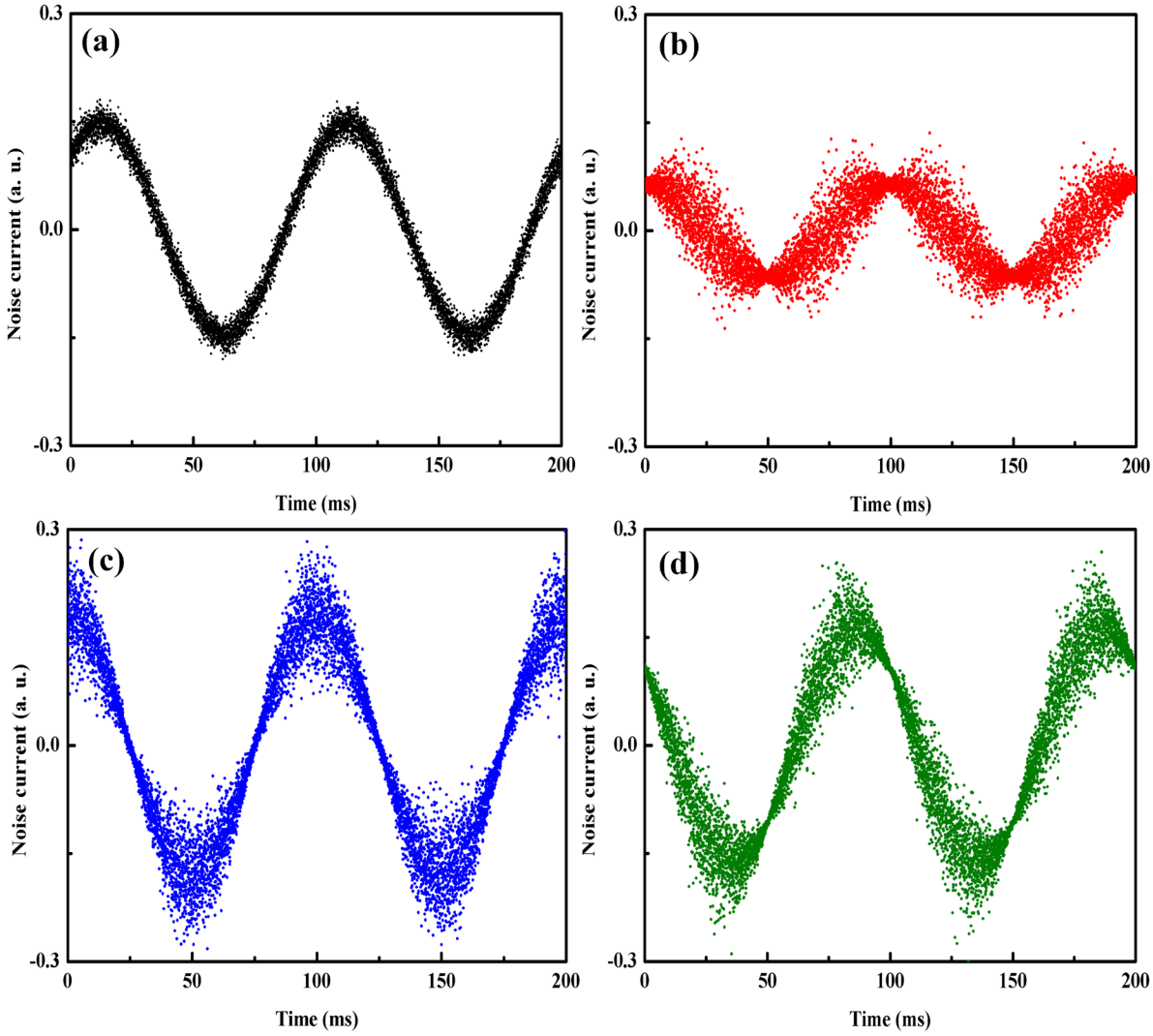

Figure 4. Noise distribution of the generated squeezed states in the time domain at a Fourier frequency of 25 MHz when the relative phase between the LO and CCF was swept from 0 to 4π in 200 ms. (a) Coherent state. (b) Amplitude-squeezed state. (c) Phase-squeezed state. (d) Squeezed state with a squeezing angle of $\pi/3$.

the change of crystal temperature led to slight detuning from resonance for the *s*-polarised squeezed states in the OPO cavity. The squeezing angle also experienced rotation by an angle dependent on detuning due to pump power fluctuation. In our experiment, the 532 nm pump light was stabilised by an MZI. The measured 532 nm laser power fluctuation was less than $\pm$ 0.1% for a given 3 h.

The measured threshold of the doubly resonant OPO was 350 mW. When the 532 nm pump power was 100 mW, the OPO was operated below the threshold and was locked by the frequency-shifted auxiliary beam using the PDH technique. Meanwhile, the CCF with 100 μW of power was injected into the subthreshold doubly resonant OPO. Because the frequency shift of the CCF from the carrier frequency was 25 MHz, which was less than the bandwidth of the OPO, the CCF could also resonate simultaneously in the OPO cavity. The OPO was turned into an OPA and bright squeezed states were generated at a Fourier frequency of 25 MHz. The reflected field of CCF from the OPO was detected by PD2 and was used to lock the relative phase between the pump field and CCF. Thus, the amplitude squeezed state, phase-squeezed state and squeezed states in an arbitrary quadrature were generated when the demodulation phase χ_1 was set to $\pi/2$, $3\pi/2$ and an arbitrary value, respectively. The generated squeezed states were measured using the BHD system with an LO power of 1.0 mW and fringe visibility between the LO and CCF of 99.4%. Figure 4 shows the noise distribution of the generated squeezed states in the time domain recorded by an OSC when the relative phase between the LO and CCF was swept from 0 to 4π in 200 ms.

Figure 4(a) shows a coherent state when the pump field of the OPO was blocked. The amplitude was proportional to the amplitude of injected CCF, and the fluctuation corresponded to the vacuum fluctuation. Figure 4(b) shows an amplitude squeezed state when the relative phase of the pump and the CCF is fixed to $\pi/2$. It can be seen that the coherent amplitude of the amplitude squeezed state is smaller than that of the coherent state (as shown in Figure 4(a)), that the noise amplitude is smaller than that of the coherent state when $\phi = 0$, π, 2π, 3π, 4π and that the noise amplitude is larger than that of

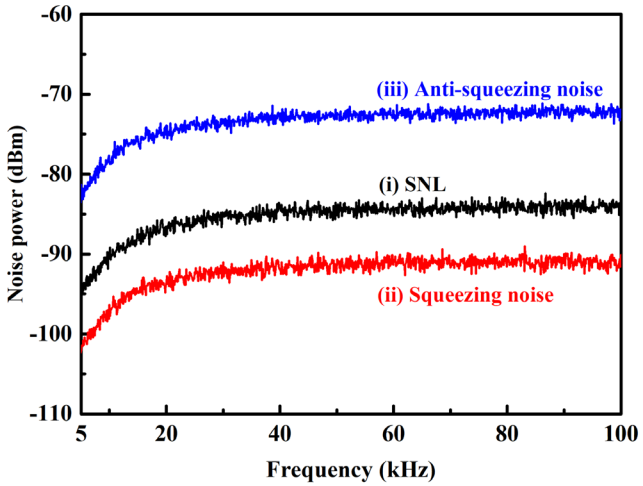

Figure 5. Measured noise power of the squeezed vacuum states at Fourier frequencies of 5–100 kHz. SA parameters: RBW of 50 Hz, VBW of 110 Hz and sweep time of 1 s. Curve (i): SNL. Curve (ii): squeezing noise. Curve (iii): anti-squeezing noise.

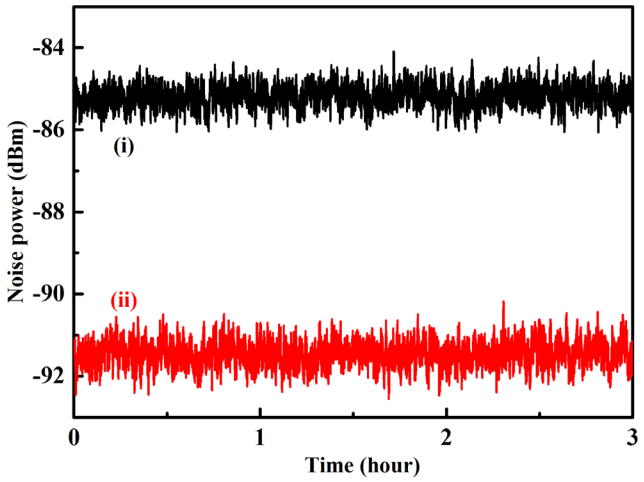

Figure 6. Measured noise power of the generated phase-squeezed vacuum states at a Fourier frequency of 20 kHz for a given 3 h. SA parameters: RBW: 50 Hz; VBW: 2 Hz. Curve (i): SNL. Curve (ii): noise power of squeezed states.

the coherent state when $\phi = \pi/2, 3\pi/2, 5\pi/2, 7\pi/2$. Figure 4(c) shows a phase-squeezed state when the relative phase of the pump and CCF is fixed to 0. It can be seen that the coherent amplitude of the phase-squeezed state is larger than that of the coherent state, that the noise amplitude is smaller than that of the coherent state when $\phi = \pi/2, 3\pi/2, 5\pi/2, 7\pi/2$ and that the noise amplitude is larger than that of the coherent state when $\phi = 0, \pi, 2\pi, 3\pi, 4\pi$. Figure 4(d) shows the noise distribution of a squeezed state in an arbitrary quadrature when the relative phase of the pump and CCF is fixed to $\pi/3$. Furthermore, a bright squeezed state in an arbitrary quadrature can be generated by controlling the value of relative phase of the pump and CCF from 0 to π. When the CCF is injected into the subthreshold OPO cavity and the relative phase between the pump field and CCF is locked, the squeezing angle of bright squeezed states at a Fourier frequency of Ω can act as a surrogate for that of the squeezed vacuum states. Consequently, squeezed vacuum states in an arbitrary quadrature can be generated by controlling the value of the relative phase of the pump and CCF from 0 to π.

When the length of the subthreshold OPO cavity was locked by the frequency-shifted auxiliary beam, the CCF was injected into the subthreshold OPO cavity and the relative phase between the pump field and CCF was locked at 0, it was possible to obtain stable, phase-squeezed vacuum states. When the relative phase between the squeezed vacuum field and LO for the BHD was fixed at $\pi/2$ by locking the relative phase between the CCF and LO at $\pi/2$, the generated phase-squeezed vacuum states could be measured continuously. Based on the fact that a home-made homodyne detector worked at audio frequencies utilising a common-mode rejection ratio (CMRR) of more than 50 dB and that an MZI was used to reduce the excess noise of the pump beam at audio-band frequencies, phase-squeezed vacuum states were measured at audio frequencies of 5 kHz to 100 kHz. Figure 5 shows the measured noise power of phase-squeezed vacuum states at Fourier frequencies of 5–100 kHz recorded by an SA with an RBW of 50 Hz, a VBW of 110 Hz and a sweep time of 1 s. Curve (i) is the SNL. Curve (ii) is the squeezing noise. Curve (iii) is the anti-squeezing noise. All noise traces were averaged 20 times. It can be seen that the measured squeezing degree of phase-squeezed vacuum states from 5 kHz to 100 kHz was approximately 6.1 ± 0.3 dB.

Figure 6 shows the measured noise power of squeezed vacuum states at a Fourier frequency of 20 kHz recorded by an SA with an RBW of 50 Hz and a VBW of 2 Hz. Curve (i) is the SNL, and curve (ii) is the noise power of the generated squeezed vacuum states. It can be seen that the generated phase-squeezed vacuum state at a frequency of 20 kHz can be measured and recorded continuously for a given 3 h.

5. Conclusion

Squeezed vacuum states were generated using a subthreshold doubly resonant OPO and a home-made, cw, single-frequency 532 nm and 1064 nm dual-wavelength Nd:YVO4/LBO laser. The subthreshold OPO was pumped by 532 nm output from the laser which was double passed through the cavity. The measured threshold of the doubly resonant OPO was 350 mW. A laser output of 1064 nm was used to generate the auxiliary beam by optical serrodyne sideband modulation via a fibre-based, waveguide-type EOPM and a nonlinear transmission line (NLTL) in order to generate the CCF by frequency shifting the 1064 nm laser using two AOMs to act as the LO beam of the BHD. When the auxiliary beam was used to lock the subthreshold OPO cavity, and the CCF beam was used to control the squeezing angle of squeezed vacuum states, as well as the relative phase between the LO field and CCF, squeezed vacuum states in an arbitrary quadrature could be stably generated with a compact configuration. When the 532 nm pump power was 100 mW, the relative phase between the pump field and CCF was locked at 0 and the relative phase between the CCF and LO was locked at $\pi/2$, the 6.1 ± 0.3 dB phase-squeezed vacuum states at audio frequencies of 5 kHz

to 100 kHz could be generated, and the generated phase-squeezed vacuum state at a frequency of 20 kHz was measured continuously for 3 h. With the help of the home-made, cw, single-frequency, dual-wavelength laser and the developed optical serrodyne sideband modulation locking method, only one laser was used to act as the pump field and as the auxiliary beam used to lock the subthreshold OPO, CCF, and LO in order to generate stable, squeezed vacuum states at audio frequency; the system was compact and low cost. Furthermore, the reduction of measured squeezing due to the relative frequency noise between the main and auxiliary lasers occurring when an auxiliary laser is used to lock the subthreshold OPO cavity can be avoided. The stable, squeezed vacuum states generated at audio frequency with a deterministic squeezing angle can be used in the field of quantum-enhanced, high-precision measurement.

Acknowledgments

This work was supported by the National Key R&D Program of China (2016YFA0301401) and the Fund for Shanxi '1331 Project' Key Subjects Construction (1331KSC).

References

[1] Caves C M 1981 Quantum-mechanical noise in an interferometer *Phys. Rev.* D **23** 1693–708
[2] Xiao M, Wu L A and Kimble H J 1987 Precision measurement beyond the shot-noise limit *Phys. Rev. Lett.* **59** 278–81
[3] Goda K, Miyakawa O, Mikhailov E E, Saraf S, Adhikari R, McKenzie K, Ward R, Vass S, Weinstein A J and Mavalvala N 2008 A quantum-enhanced prototype gravitational-wave detector *Nat. Phys.* **4** 472–6
[4] Gong L H, Li J F and Zhou N R 2018 Continuous variable quantum network dialogue protocol based on single-mode squeezed states *Laser Phys. Lett.* **15** 105204
[5] Brida G, Genovese M and Berchera I R 2010 Experimental realization of sub-shot-noise quantum imaging *Nat. Photon.* **4** 227–30
[6] Treps N, Grosse N, Bowen W P, Fabre C and Bachor H A 2003 A quantum laser pointer *Science* **301** 940–43
[7] Taylor M A, Janousek J, Daria V, Knittel J, Hage B, Bachor H A and Bowen W P 2013 Biological measurement beyond the quantum limit *Nat. Photon.* **7** 229–33
[8] Wu L A, Kimble H J, Hall J L and Wu H F 1986 Generation of squeezed states by parametric down conversion *Phys. Rev. Lett.* **57** 2520–3
[9] Serikawa T, Yoshikawa J, Makino K and Furusawa A 2016 Creation and measurement of broadband squeezed vacuum from a ring optical parametric oscillator *Opt. Express* **24** 28383–91
[10] Yang W H, Shi S P, Wang Y J, Ma W G, Zheng Y H and Peng K C 2017 Detection of stably bright squeezed light with the quantum noise reduction of 12.6dB by mutually compensating the phase fluctuations *Opt. Lett.* **42** 4553–6
[11] Wan Z J, Feng J X, Li Y J and Zhang K S 2018 Comparison of phase quadrature squeezed states generated from degenerate optical parametric amplifiers using PPKTP and PPLN *Opt. Express* **26** 5531–40
[12] Pérez A M, Just F, Cavanna A, Chekhova M V and Leuchs G 2013 Compensation of anisotropy effects in a nonlinear crystal for squeezed vacuum generation *Laser Phys. Lett.* **10** 125201
[13] Vahlbruch H, Mehmet M, Danzmann K and Schnabel R 2016 Detection of 15 dB squeezed states of light and their application for the absolute calibration of photoelectric quantum efficiency *Phys. Rev. Lett.* **117** 110801
[14] Heurs M, Petersen I R, James M R and Huntington E H 2009 Homodyne locking of a squeezer *Opt. Lett.* **34** 2465–7
[15] Drever R W P, Hall J L, Kowalski F V, Hough J, Ford G M, Munley A J and Ward H 1983 Laser phase and frequency stabilization using an optical resonator *Appl. Phys.* B **31** 97–105
[16] McKenzie K, Grosse N, Bowen W P, Whitcomb S E, Gray M B, McClelland D E and Lam P K 2004 Squeezing in the audio gravitational-wave detection band *Phys. Rev. Lett.* **93** 161105
[17] Vahlbruch H, Chelkowski S, Hage B, Franzen A, Danzmann K and Schnabel R 2006 Coherent control of vacuum squeezing in the gravitational-wave detection band *Phys. Rev. Lett.* **97** 011101
[18] The LIGO Scientific Collaboration 2011 A gravitational wave observatory operating beyond the quantum shot-noise limit *Nat. Phys.* **7** 962–5
[19] Johnson L M and Cox C H 1988 Serrodyne optical frequency translation with high sideband suppression *IEEE J. Lightwave Technol.* **6** 109–12
[20] Houtz R, Chan C and Müller H 2009 Wideband efficient optical serrodyne frequency shifting with a phase modulator and a nonlinear transmission line *Opt. Express* **17** 19235–40
[21] Khalaidovski A, Vahlbruch H, Lastzka N, Gräf C, Danzmann K, Grote H and Schnabel R 2012 Long-term stable squeezed vacuum state of light for gravitational wave detectors *Class. Quantum Grav.* **29** 075001
[22] Oelker E, Mansell G, Tse M, Miller J, Matichard F, Barsotti L, Fritschel P, McClelland D E, Evans M and Mavalvala N 2016 Ultra-low phase noise squeezed vacuum source for gravitational wave detectors *Optica* **3** 682–5
[23] Edgar V, Olaf O, Burkhard S and Andreas N 1982 Optical phase and amplitude measurement by single sideband homodyne detection *IEEE J. Quantum Electron.* **18** 124–9
[24] Chelkowski S, Bahlbruch H, Danzmann K and Schnabel R 2007 Coherent control of broadband vacuum squeezing *Phys. Rev.* A **75** 043814
[25] Khalaidovski A 2011 Beyond the quantum limit *PhD Thesis* Gottfried Wilhelm Leibniz University, Hannover (http://inspirehep.net/record/1251637/files/khalaidovski_thesis.pdf)
[26] Afshari E and Hajimiri A 2005 Non-linear transmission line for pulse shaping in silicon *IEEE J. Solid-State Circuits* **40** 744–52